

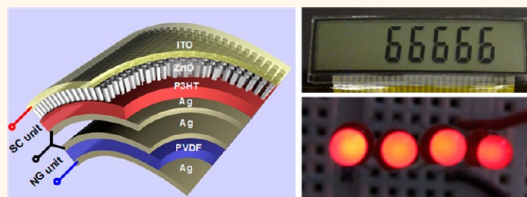
Flexible Hybrid Energy Cell for Simultaneously Harvesting Thermal, Mechanical, and Solar Energies

Ya Yang,[†] Hulin Zhang,[†] Guang Zhu,[†] Sangmin Lee,[†] Zong-Hong Lin,[†] and Zhong Lin Wang^{†,*,‡}

[†]School of Materials Science and Engineering, Georgia Institute of Technology, Atlanta, Georgia 30332-0245, United States and

[‡]Beijing Institute of Nanoenergy and Nanosystems, Chinese Academy of Sciences, Beijing, China

ABSTRACT We report the first flexible hybrid energy cell that is capable of simultaneously or individually harvesting thermal, mechanical, and solar energies to power some electronic devices. For having both the pyroelectric and piezoelectric properties, a polarized poly(vinylidene fluoride) (PVDF) film-based nanogenerator (NG) was used to harvest thermal and mechanical energies. Using aligned ZnO nanowire arrays grown on the flexible polyester (PET) substrate, a ZnO–poly(3-hexylthiophene) (P3HT) heterojunction solar cell was designed for harvesting solar energy. By integrating the NGs and the solar cells, a hybrid energy cell was fabricated to simultaneously harvest three different types of energies. With the use of a Li-ion battery as the energy storage, the harvested energy can drive four red light-emitting diodes (LEDs).



KEYWORDS: pyroelectric · piezoelectric · nanogenerator · solar cell · ZnO · PVDF

The purpose of self-powered nanotechnology is to harvest energy in the living environment to power small electronic devices.^{1–3} Usually, we can obtain the thermal, mechanical, and solar energies from our living environment. Harvesting these types of energies is of critical importance for our long-term energy needs and sustainable development.⁴ However, these energies are not always available at the same time, depending on day/night, the weather, working conditions, and some other cases. The concept of a hybrid energy cell is to develop a technology to simultaneously/individually harvest these energies by using an integrated device,^{5,6} so that the devices can be powered by using whatever energy that is available at their working environment. Although some attempts at hybrid energy cells for scavenging two kinds of energies have been achieved,^{7,8} there has been no report about a hybrid energy cell that can simultaneously harvest thermal, mechanical, and solar energies. This multimode energy harvesting cell has potential applications for driving micro/nanosystems.

Currently, pyroelectric nanogenerators (NGs) have been demonstrated as a potential approach for converting thermal energy

into electricity from a time-dependent temperature fluctuation.^{9,10} The piezoelectric NGs have been extensively used to harvest mechanical energy.^{11–13} The nanowire-based solar cells can be used to convert solar energy into electric energy.^{14,15} Usually, the materials used for the different NGs are different, and the methodologies are different, as well. However, for some materials, such as ZnO, PZT, and PVDF that have both the pyroelectric and piezoelectric properties, they can be used for fabricating both the pyroelectric and piezoelectric NGs.^{16–18} These multifunctional energy materials are important for fabricating the hybrid energy cells since they can save the fabrication cost and decrease the total size of the hybrid energy cell. In this paper, we demonstrate a flexible hybrid energy cell for simultaneously/individually harvesting thermal, mechanical, and solar energies. A PVDF-based pyro/piezoelectric NG was built on its bottom surface for harvesting thermal and mechanical energies, which can directly drive a LCD by using hand touching. A ZnO nanowire array–P3HT film heterojunction solar cell was built on the top surface to harvest solar energy. The hybrid energies produced by the NG and solar cells can be stored in a Li-ion battery,

* Address correspondence to zlwang@gatech.edu.

Received for review November 11, 2012 and accepted December 2, 2012.

Published online December 03, 2012
10.1021/nn305247x

© 2012 American Chemical Society

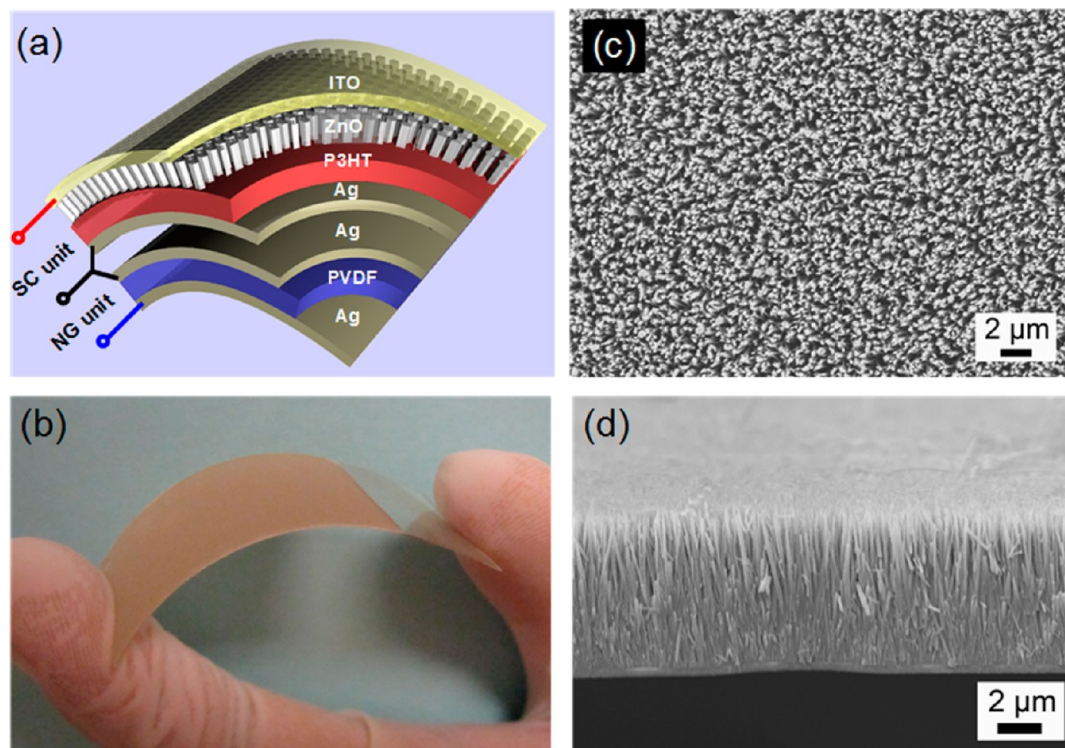


Figure 1. (a) Schematic diagram of the fabricated hybrid energy cell. (b) Photograph of the bent ZnO nanowire array grown on an ITO/PET substrate. (c) SEM image of the ZnO nanowire array. (d) Cross-section SEM image of the ZnO nanowire array.

which can drive four red LEDs. Our study demonstrates an innovative approach for developing integrated energy technologies for powering micro/nanosystems.

RESULTS AND DISCUSSION

Figure 1a shows a schematic of the fabricated hybrid energy cell. All of the materials used for the fabrication are flexible. The bottom pyroelectric/piezoelectric NG consists of two Ag electrodes and PVDF film. The optical images of the fabricated PVDF film-based pyroelectric/piezoelectric NG are shown in Figure S1 of the Supporting Information, indicating that the NG can be bent and the surface area is about 600 mm². A cross-section SEM image of the PVDF film in Figure S2 shows that the thickness is about 110 μm. The micrometer size PVDF film was chosen for easy manipulation and just as a model system in the hybrid energy cell for this study. The top solar cell device consists of a transparent indium tin oxide (ITO) film electrode, ZnO nanowire array, P3HT film, and Ag electrode. In this study, in order to avoid the temperature fluctuation effect on the performance of solar cells, the Ag films between PVDF and P3HT were separated. Figure 1b shows an optical image of a bent ZnO nanowire array grown on the ITO/PET substrate, indicating a large flexibility of the device. The ZnO nanowire arrays were obtained by using a simple solution-based growth technique. The detailed growth method is given in Experimental Section. Figure 1c shows a scanning

electron microscopy (SEM) image of the ZnO nanowire array, revealing that the diameters of the ZnO nanowires are about 100 nm. The cross-section SEM image of the ZnO nanowire array in Figure 1d shows that the length is about 10 μm.

We first measured the voltage/current output of the PVDF film-based pyroelectric NG for harvesting thermal energy. Figure 2a shows the cyclic changes in temperature of the pyroelectric NG and the corresponding differential curve. Under the forward connection to the measurement system, a negative voltage/current pulse (−2.5 V/−24 nA) was observed when the temperature was increased from 295 to 314 K, as shown in Figure 2b. When the temperature was returned to 295 K, there was a positive voltage/current pulse (3.2 V/31 nA), which is slightly larger than that of the negative pulse due to the larger temperature changing rate. The NG was reversely connected to the measurement system, and the output voltage and current are shown in Figure 2c. The obtained opposite signals indicate that the measured data were generated by the fabricated NG. According to pyroelectric theory, the pyroelectric current I_p can be given by

$$I_p = pA \frac{dT}{dt} \quad (1)$$

where p is pyroelectric coefficient, A is the electrode area, and dT/dt is the temperature changing rate.¹⁹ By using the experimental data, we estimated a

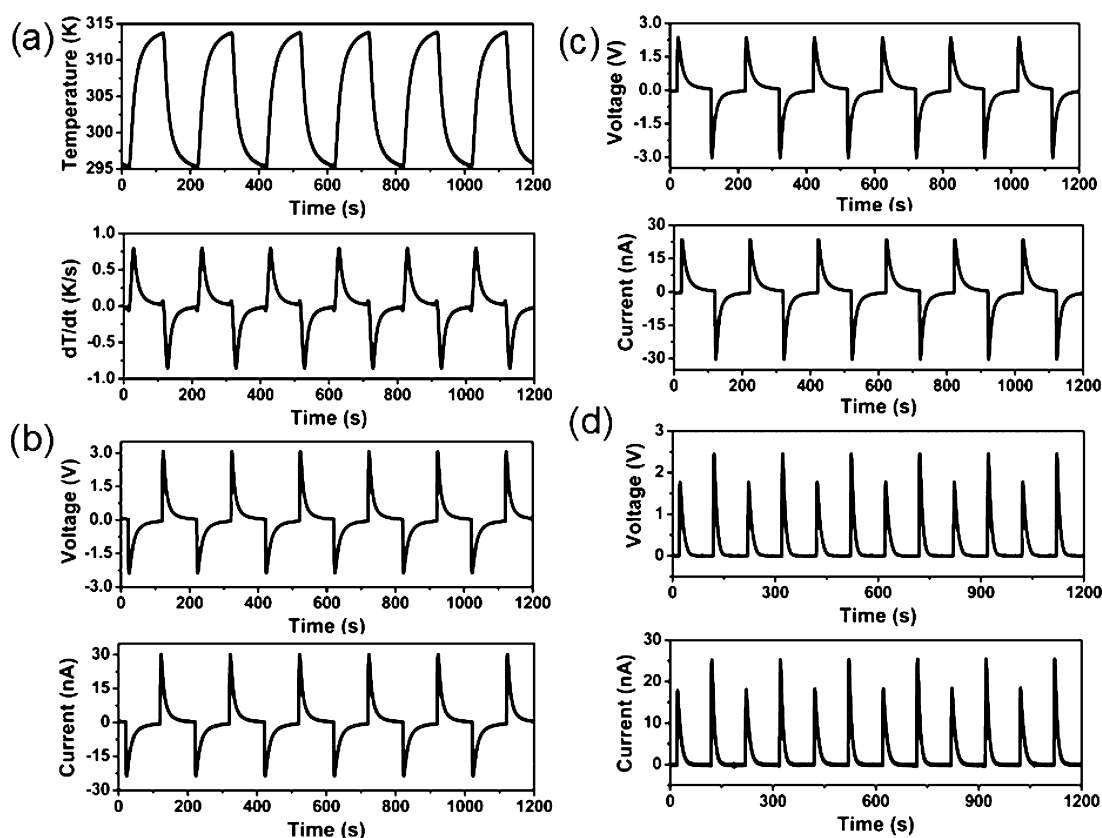


Figure 2. (a) Cyclic changes in temperature of a PVDF film-based pyroelectric nanogenerator and the corresponding differential curve. (b,c) Measured output voltage and current of the device under the forward (b) and reversed (c) connection conditions when it was subject to a cyclic temperature change in (a). (d) Measured output voltage and current of the device after rectification.

pyroelectric coefficient of about $-44 \mu\text{C}/\text{m}^2 \text{K}$, which is much larger than those of the reported ZnO and KNbO_3 materials-based pyroelectric NGs.^{9,10} The pyroelectric voltage V_p can be simply expressed as

$$V_p = \frac{pd\Delta T}{(\epsilon_r - 1)\epsilon_0} \quad (2)$$

where d is the thickness of the film, ΔT is the change in temperature, ϵ_r is the relative dielectric constant of the sample, and ϵ_0 is the permittivity of free space.²⁰ According to eqs 1 and 2, when the temperature of the NG is increased, a negative pyroelectric voltage output signal should be observed under the forward connection to the measurement system due to the negative pyroelectric coefficient, which is consistent with the experimental data shown in Figure 2b. Both the pyroelectric current and voltage can be enhanced by increasing the pyroelectric coefficient of the NG. The alternating electric output signals of the pyroelectric NG in Figure 2b, c can be rectified by a full-wave bridge circuit, resulting in all output voltage/current pulses being positive in Figure 2d, which is important for driving some polar electronic devices. The values of the rectified output voltage and current are nearly the same as those before the rectification in Figures 2b,c.

We also demonstrated that the same PVDF film-based NG can be used to harvest mechanical energy. Figure 3a shows the output voltage and current of the PVDF film-based piezoelectric NG. When a compressive strain was applied on the NG, a positive voltage/current pulse (0.5 V/20 nA) was observed under the forward connection to the measurement system, as shown in Figure 3a. After the compressive strain was released, a negative voltage/current pulse appeared. Piezoelectric output pulses with opposite sign were obtained by switching the polarity for electric measurement, as shown in Figure 3b. The peak width of the piezoelectric output signals is much smaller than that of the pyroelectric output signals in Figure 2. Figure 3c shows the hybrid pyroelectric and piezoelectric output voltage/current by using the PVDF film-based NG, demonstrating its capability of simultaneously and individually harvesting thermal and mechanical energies. The output signals of hybrid NGs look different from the measured signals of two individual NGs, which is associated with the heat-induced deformation of PVDF. Usually, when the NG was touched by a hand, the temperature of NG was increased and a compressed strain was created in the NG. The hybrid pyroelectric and piezoelectric NGs can be used to directly drive a LCD (with a display of "66666"), as shown in

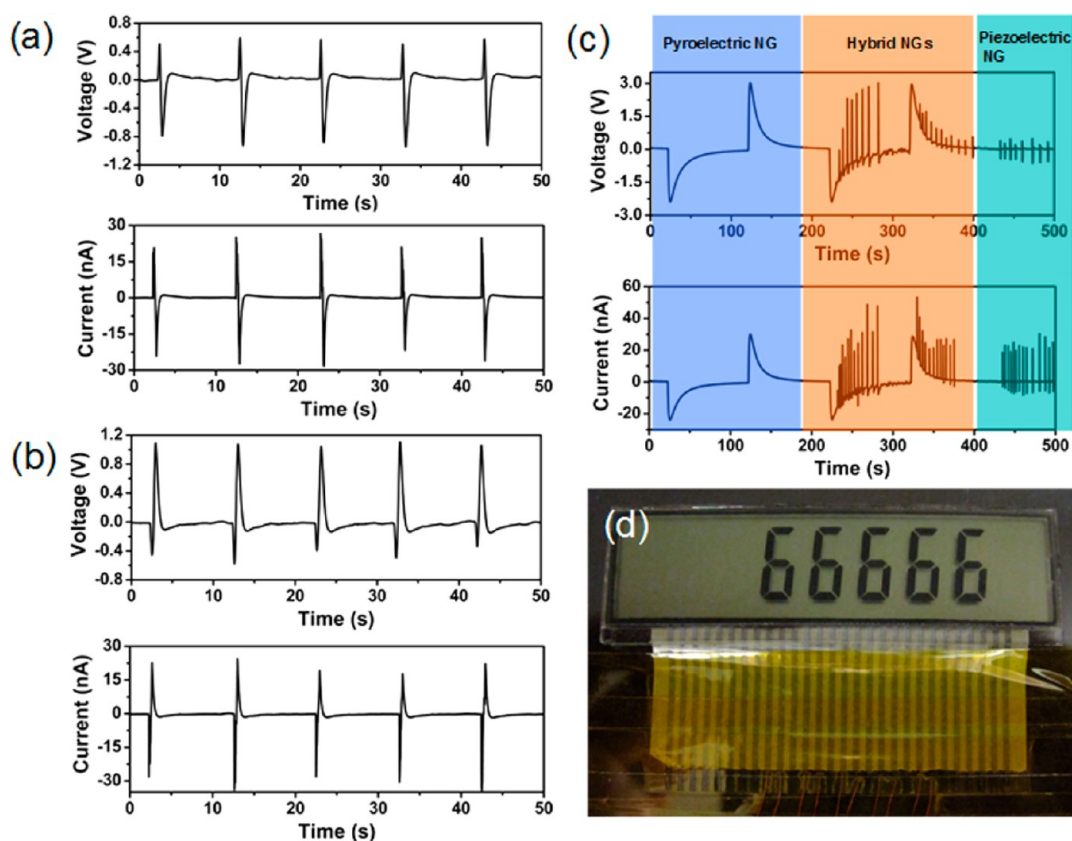


Figure 3. (a,b) Measured output voltage and current of the PVDF film-based piezoelectric nanogenerator under the forward (a) and reversed (b) connection conditions. (c) Output voltage and current of the hybrid pyroelectric and piezoelectric NGs. (d) Optical image of a LCD driven by the hybrid thermal and mechanical energies, which was induced by hand touch.

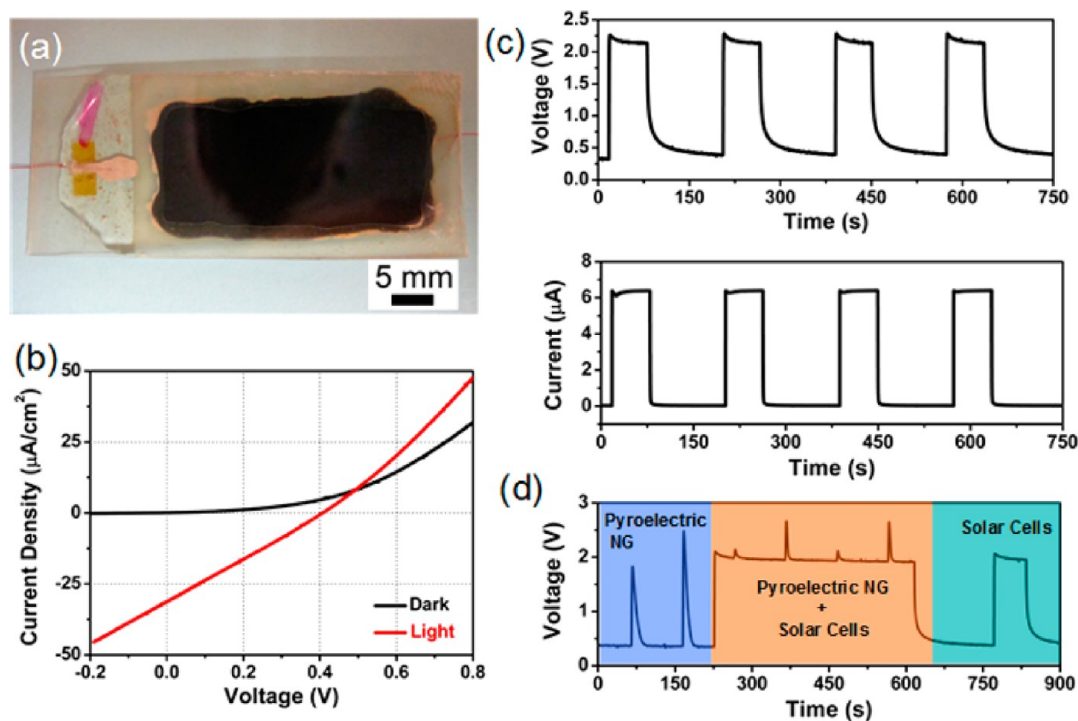


Figure 4. (a) Photograph of the fabricated ZnO nanowire array-P3HT film solar cell. (b) I - V characteristics of the device under dark and light illumination conditions. (c) Output voltage and current of the integrated six solar cells in serial connection. (d) Output voltage of the hybrid pyroelectric (after rectification) and solar cells for harvesting thermal and solar energies.

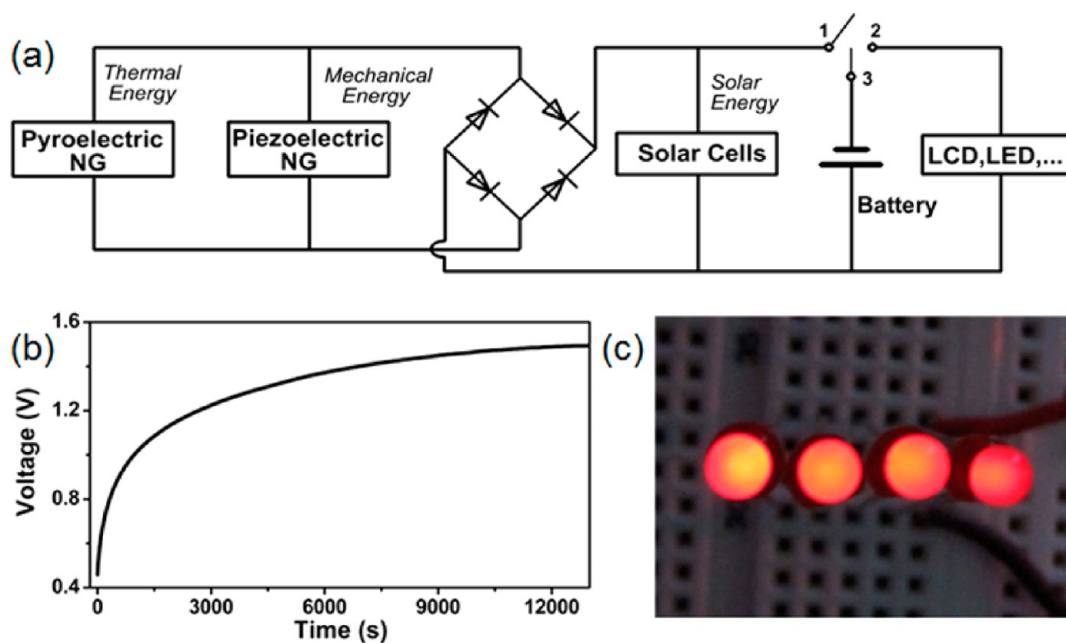


Figure 5. (a) Schematic diagram of the hybrid energy cell, which includes the pyroelectric nanogenerator, the piezoelectric nanogenerator, and the solar cells in parallel connection. (b) V - T charging curve of a Li-ion battery by using the hybrid NG and solar cells. (c) Optical image of four red LEDs driven by the charged Li-ion battery.

Figure 3d. The video in the Supporting Information shows that the LCD can be driven when the hybrid energy cell was touched by a hand.

In order to use the fabricated hybrid energy cell to harvest solar energy, the flexible ZnO nanowire array-P3HT film heterojunction solar cell was fabricated. Figure 4a shows the optical image of the fabricated solar cell, where the dark area was covered by a P3HT film. Figure 4b shows a photovoltaic performance of the device under dark and light illumination conditions. Under AM 1.5 illumination with 100 mW/cm^2 light intensity, the open-circuit voltage of the solar cell is about 0.41 V and the short-circuit current density is $31 \mu\text{A/cm}^2$. To increase the output voltage of the device, six solar cells were connected in sequence (in Figure S3), which gave an output voltage of about 2 V and an output current of about $6 \mu\text{A}$, as shown in Figure 4c. The obtained output voltage/current signals can be switched in sign when reversely connected to the measurement system, as shown in Figure S4. Figure 4d shows the hybrid output voltage of the solar cell and the pyroelectric NG, where the pyroelectric output signals were rectified. The schematic diagram of the measurement circuit is shown in Figure S5. It can be seen that the pyroelectric NG and the solar cells can work simultaneously and individually to harvest thermal and solar energies, respectively.

Figure 5a shows a schematic diagram of the integrated hybrid energy cell, where the pyroelectric and piezoelectric NGs were connected with a bridge rectification circuit (Figure S5) for converting alternating current (ac) to direct current (dc) signals. The NGs and the solar cells were connected in parallel, which can

ensure that there is always a voltage/current output when either the thermal or mechanical, or solar energy is available. The hybrid energy cell can work to directly drive some small electric devices (such as LCD in Figure 3d) when the point "1" was connected to the point "2". Moreover, the hybrid energies can also be stored in a Li-ion battery when the point "1" is connected to the point "3". Figure 5b shows the charging curve of the Li-ion battery by using the hybrid NG and solar cells, where the voltage of the Li-ion battery can be charged to about 1.5 V . It can be used to drive four red LEDs in parallel connection, as shown in Figure 5c. The purpose of designing the hybrid energy cell is to ensure that the powering devices can harvest thermal/mechanical/solar energy that is available in our living environment.

CONCLUSION

In summary, we have developed the first fully integrated flexible hybrid energy cell that consists of a pyroelectric NG, a piezoelectric NG, and a solar cell, which can be used to simultaneously/individually harvest thermal, mechanical, and solar energies. Pyro/piezoelectric NGs are based on a flexible PVDF film with both pyroelectric and piezoelectric properties, which can be used to drive a LCD by using the hand-touching-induced hybrid thermal and mechanical energies. The solar cell device was designed by using a flexible ZnO nanowire array-P3HT film heterojunction, which can give an output voltage of 0.41 V and an output current density of $31 \mu\text{A/cm}^2$. The hybrid energies were stored in a Li-ion battery, which can be used to drive four red LEDs in parallel connection. The

hybrid energy cells developed here have potential applications in wireless sensor systems, medical

diagnostics, environmental surveillance, and defense technology.

EXPERIMENTAL SECTION

Fabrication of the ZnO Nanowire Array. First, an aqueous solution of hexamethylenetetramine (HMTA) and zinc chloride (ZnCl_2) in equal concentrations (20 mM) was used in the growth of the ZnO nanowire array. Ammonium hydroxide (NH_4OH) was added into the solution, where the volume concentration is about 5%. A transparent PET substrate was sputtered with a layer of ITO film with a thickness of about 300 nm, which was used as the conductive electrode. A ZnO seed layer with a thickness of about 50 nm was then covered on the ITO surface. The substrate was fixed on a glass substrate and was then put facing downward into the growth solution, which was put in a Yamato convection box oven at 368 K for 8 h.

Fabrication and Measurement of the Hybrid Energy Cell. The pyroelectric and piezoelectric NGs were fabricated by using a polarized PVDF film, which has both pyroelectric and piezoelectric properties. The solar cell device was fabricated by using the ZnO nanowire array–P3HT film heterojunction, where the ITO and Ag films were used as the electrodes. The solar cell was irradiated at the transparent ITO side by using a solar simulator (500 W model 91160, Newport) with an AM 1.5 spectrum distribution calibrated against a reference cell to simulate accurately a full-sun intensity (100 mW/cm^2). The thermoelectric-based heater was used to change the temperature of the device. A temperature sensor was used to record the temperature of the pyroelectric NG. The light was illuminated on the top solar cells, and the temperature changes/external forces were applied on the bottom pyroelectric/piezoelectric NGs when the pyroelectric, piezoelectric, and solar cells were integrated. The output voltage and current of the fabricated hybrid energy cell were measured by using a low-noise voltage preamplifier (Stanford Research System model SR560) and a low-noise current preamplifier (Stanford Research System model SR570).

Conflict of Interest: The authors declare no competing financial interest.

Acknowledgment. This work was supported by Airforce, MURI, U.S. Department of Energy, Office of Basic Energy Sciences (DE-FG02-07ER46394), NSF, National Institute For Materials, Japan (Agreement DTD 1 Jul. 2008), Samsung, and the Knowledge Innovation Program of the Chinese Academy of Sciences (KJCX2-YW-M13).

Supporting Information Available: (1) Optical image of the fabricated pyroelectric/piezoelectric NG, (2) cross-section SEM image of the fabricated NG, (3) optical image of the integrated six solar cells, (4) output voltage and current of the integrated solar cells under the reversed connection to the measurement system, (5) schematic diagram of the measurement circuit of the hybrid pyroelectric NG and solar cells. The additional movie file is to drive a LCD by using the hybrid thermal and mechanical energies induced by a hand touching. This material is available free of charge via the Internet at <http://pubs.acs.org>.

REFERENCES AND NOTES

- Xu, S.; Qin, Y.; Xu, C.; Wei, Y.; Yang, R.; Wang, Z. L. Self-Powered Nanowire Devices. *Nat. Nanotechnol.* **2010**, *5*, 366–373.
- Wang, Z. L. Toward Self-Powered Sensor Networks. *Nano Today* **2010**, *5*, 512–514.
- Lee, M.; Bae, J.; Lee, J.; Lee, C.-S.; Hong, S.; Wang, Z. L. Self-Powered Environmental Sensor System Driven by Nanogenerators. *Energy Environ. Sci.* **2011**, *4*, 3359–3363.
- Dresselhaus, M. S.; Thomas, I. L. Alternative Energy Technologies. *Nature* **2001**, *414*, 332–337.
- Xu, C.; Wang, Z. L. Compacted Hybrid Cell Made by Nanowire Convolved Structure for Harvesting Solar and Mechanical Energies. *Adv. Mater.* **2011**, *23*, 873–877.
- Guo, X.-Z.; Zhang, Y.-D.; Qin, D.; Luo, Y.-H.; Li, D.-M.; Pang, Y.-T.; Meng, Q.-B. Hybrid Tandem Solar Cell for Concurrently Converting Light and Heat Energy with Utilization of Full Solar Spectrum. *J. Power Sources* **2010**, *195*, 7684–7690.
- Pan, C.; Guo, W.; Dong, L.; Zhu, G.; Wang, Z. L. Optical Fiber-Based Core-Shell Coaxially Structured Hybrid Cells for Self-Powered Nanosystems. *Adv. Mater.* **2012**, *24*, 3356–3361.
- Xu, C.; Wang, X.; Wang, Z. L. Nanowire Structured Hybrid Cell for Concurrently Scavenging Solar and Mechanical Energies. *J. Am. Chem. Soc.* **2009**, *131*, 5866–5872.
- Yang, Y.; Guo, W.; Pradel, K. C.; Zhu, G.; Zhou, Y.; Zhang, Y.; Hu, Y.; Lin, L.; Wang, Z. L. Pyroelectric Nanogenerators for Harvesting Thermoelectric Energy. *Nano Lett.* **2012**, *12*, 2833–2838.
- Yang, Y.; Jung, J. H.; Yun, B. K.; Zhang, F.; Pradel, K. C.; Guo, W.; Wang, Z. L. Flexible Pyroelectric Nanogenerators Using a Composite Structure of Lead-Free KNbO_3 Nanowires. *Adv. Mater.* **2012**, *24*, 5357–5362.
- Chang, C.; Tran, V. H.; Wang, J.; Fuh, Y.-K.; Lin, L. Direct-Write Piezoelectric Polymeric Nanogenerator with High Energy Conversion Efficiency. *Nano Lett.* **2010**, *10*, 726–731.
- Chen, X.; Xu, S.; Yao, N.; Shi, Y. 1.6 V Nanogenerator for Mechanical Energy Harvesting Using PZT Nanofibers. *Nano Lett.* **2010**, *10*, 2133–2137.
- Zhu, G.; Wang, A. C.; Liu, Y.; Zhou, Y.; Wang, Z. L. Functional Electrical Stimulation by Nanogenerator with 58 V Output Voltage. *Nano Lett.* **2012**, *12*, 3086–3090.
- Tian, B.; Zheng, X.; Kempa, T. J.; Fang, Y.; Yu, N.; Yu, G.; Huang, J.; Lieber, C. M. Coaxial Silicon Nanowires as Solar Cells and Nanoelectronic Power Sources. *Nature* **2007**, *449*, 885–890.
- Kempa, T. J.; Tian, B.; Kim, D. R.; Hu, J.; Zheng, X.; Lieber, C. M. Single and Tandem Axial p-i-n Nanowire Photovoltaic Devices. *Nano Lett.* **2008**, *8*, 3456–3460.
- Zook, J. D.; Liu, S. T. Pyroelectric Effects in Thin Film. *J. Appl. Phys.* **1978**, *49*, 4604–4606.
- Lang, S. B. Pyroelectricity: From Ancient Curiosity to Modern Imaging Tool. *Phys. Today* **2005**, *58*, 31–36.
- Ploss, B.; Ploss, B.; Shin, F. G.; Chan, H. L. W.; Choy, C. L. Pyroelectric or Piezoelectric Compensated Ferroelectric Composites. *Appl. Phys. Lett.* **2000**, *76*, 2776–2778.
- Ye, C.; Tamagawa, T.; Polla, D. L. Experimental Studies on Primary and Secondary Pyroelectric Effects in $\text{Pb}(\text{Zr}_x\text{Ti}_{1-x})\text{O}_3$, PbTiO_3 , and ZnO Thin Films. *J. Appl. Phys.* **1991**, *70*, 5538–5543.
- Wen, S.; Chung, D. D. L. Pyroelectric Behavior of Cement-Based Materials. *Cem. Concr. Res.* **2003**, *33*, 1675–1679.